frontiers in Chemistry

ORIGINAL RESEARCH
published: 17 April 2019
doi: 10.3389/fchem.2019.00142

Nitrogen Doped Carbons Derived From Graphene Aerogel Templated Triazine-Based Conjugated Microporous Polymers for High-Performance Supercapacitors

Lan Peng[1,2], *Qianyin Guo*[1,2], *Zhaolin Ai*[1,2], *Yan Zhao*[2,3], *Yunqi Liu*[2,3] *and Dacheng Wei*[1,2]*

[1] State Key Laboratory of Molecular Engineering of Polymers, Department of Macromolecular Science, Fudan University, Shanghai, China, [2] Institute of Molecular Materials and Devices, Fudan University, Shanghai, China, [3] Department of Material Sciences, Fudan University, Shanghai, China

Conjugated microporous polymers (CMPs) have attracted intensive attention owing to their permanent nanoporosity, large surface area and possibility for functionalization, however their application in energy storage suffers from poor conductivity and low hetero-atom content. Here, we demonstrate a hybrid of conjugated microporous polymers and graphene aerogel with improved conductivity. After treating at 800°C in NH_3, the nitrogen content increases to 9.8%. The resulting microporous carbon exhibits a significant rise in supercapacitive performance up to 325 F g^{-1}, 55% higher than pristine triazine-based CMPs, with energy density up to 12.95 Wh kg^{-1}. Moreover, it has high stability with 99% retention after 10,000 cycles at 5 A g^{-1}. The synergy of hierarchical porous structure, graphene-based conduction path and high percentage of hybridization with nitrogen ensures effective ion/electron transport and diffusion, making NH_3-treated graphene aerogel/CMP hybrid a promising electrode material in high-performance supercapacitor.

Keywords: conjugated microporous polymer, graphene aerogel, supercapacitors, triazine-based electrode materials, nitrogen-doped carbon

OPEN ACCESS

Edited by:
Penglei Chen,
Institute of Chemistry (CAS), China

Reviewed by:
Xiaodong Zhuang,
Shanghai Jiao Tong University, China
Bao-Hang HAN,
National Center for Nanoscience and Technology (CAS), China
Huiqiao Li,
Huazhong University of Science and Technology, China

***Correspondence:**
Dacheng Wei
weidc@fudan.edu.cn

Specialty section:
This article was submitted to Supramolecular Chemistry, a section of the journal Frontiers in Chemistry

Received: *25 November 2018*
Accepted: *26 February 2019*
Published: *17 April 2019*

Citation:
Peng L, Guo Q, Ai Z, Zhao Y, Liu Y and Wei D (2019) Nitrogen Doped Carbons Derived From Graphene Aerogel Templated Triazine-Based Conjugated Microporous Polymers for High-Performance Supercapacitors. Front. Chem. 7:142. doi: 10.3389/fchem.2019.00142

INTRODUCTION

Conjugated microporous polymers (CMPs) are one kind of covalently linked organic porous materials which have attracted extensive interest in recent years due to their strong π-conjugated linkage, permanent nanoporosity, large surface area, possibility to modify functional groups as well as high stability compared with other porous organic materials (Xu et al., 2013). Until now, CMPs have been used in various fields, including gas adsorption and storage (Yuan et al., 2010; Reich et al., 2012), gas separation, heterogeneous catalysis, light harvesting devices, photoluminescence, electric energy conversion and storage, etc. Among them, supercapacitor, as one kind of electrochemical energy storage devices, shows great potential for daily appliances (Pang et al., 2015; Zhang et al., 2015, 2016; Xie and Zhang, 2016) owing to its fast charge-discharge rate, high power density, less environment pollution, etc. (Zhang and Zhao, 2009; Wang G. et al., 2012; Peng et al., 2014; Salunkhe et al., 2014; Wang Q. et al., 2014)Compared with traditional supercapacitor electrode materials, CMPs have high specific surface area and the possibility to tailor pore and channel structures. Recently, the CMPs are normally produced by solvothermal method, which is

suitable for carbon-carbon bond-forming reactions. However, CMPs produced by solvothermal method have relatively poor orbital overlap due to the twisted benzene rings, leading to low electrical conductivity (Lee et al., 2016). To improve the conductivity, CMPs with high carbon content are synthesized by coupling reactions, however it usually results in poor wettability of CMPs-based electrode.

To improve the performance of CMPs as electrode material, hybridization with other heteroatoms are widely used, which can increase both the wettability and the pseudocapacitance. With higher nitrogen content, the supercapacitive performance of a triazatruxene-functional CMP are remarkably improved, however the value only reaches 183 F g^{-1} (Li et al., 2017). Moreover, to increase the material conductivity, CMPs are usually carbonized under high temperature, which graphitizes the framework of carbon-based materials (Li et al., 2014; Wang L. et al., 2014). As an example, Cooper et al. improve the electrical conductivity and pseudocapacitive contributions of CMPs by combining molecular design and carbonization under an ammonia atmosphere, however the value only increased to about 260 F g^{-1} and the performance still restricts by the limited intrinsic conductivity of CMPs, which is also a common problem for other porous organic electrode materials (Lee et al., 2016).

Here, graphene aerogels (GA) are hybridized with CMPs, for the first time, to improve three-dimensional intrinsic conductivity of CMPs. After carbonization under ammonia atmosphere, the nitrogen content increases to 9.8%, while the ratio of pyridinic nitrogen increase from 15 to 25.5%. Owing to the improved electrical conductivity and higher nitrogen content, the resulting NH_3-treated GA/CMPs (N-GA /CMPs) has extraordinary specific capacitance up to 325 F g^{-1} at 0.5 A g^{-1} with excellent long-term cycling stability, showing its great potential in high performance supercapacitors.

MATERIALS AND METHODS

Preparation of CMP, GA/CMP, N-GA/CMP

CMPs were synthesized by the ionothermal method (Kuhn et al., 2008a). The proportional (1:20) monomer (m-phthalodinitrile) and $ZnCl_2$ were added to a Pyrex ampoule in an argon atmosphere, and then the ampoule was evacuated and sealed. With a 10°C min^{-1} heating rate, the ampoule was heated to 600°C for 40 h, and then was cooled down to room temperature. If the synthesis temperature was higher than 500°C, the ampule was under pressure and would be released during opening (Kuhn et al., 2008b). The product was subsequently grounded in an agate mortar to get powder, and washed by deionized water to remove $ZnCl_2$. After that, the sample was stirred in 5% HCl for 15 h to remove the residual $ZnCl_2$. After purification, the black powder was filtered and washed with deionized water and tetrahydrofuran. Finally, it was dried in vacuum at 150°C for 15 h. Graphene oxide was synthesized from natural graphite according to a modified Hummers method (Hummers Jr and Offeman, 1958). The prepared graphene oxide solution was purified by 5% HCl and deionized water for several times so that residual salts and acids can be washed completed. Graphene Aerogel was synthesized according to the literature (Xu et al., 2010). A 10 mL portion of 1.5 mg mL^{-1} homogeneous graphene oxide aqueous dispersion was sealed in a 20 mL Teflon-lined autoclave and maintained at 180°C for 12 h. The autoclave was naturally cooled to room temperature, and the as-prepared graphene aerogels were taken out and transferred to glass bottles. The graphene aerogels were obtained by putting the glass bottles into a freeze drying equipment for 24 h. The preparation of GA/CMPs followed the preparation of CMPs but different ratio of graphene aerogels, monomers and $ZnCl_2$ were grinded evenly in an agate mortar before adding to a Pyrex ampoule. The weight percentage of GA was 15%. To prepare N-GA/CMP, GA/CMPs (200 mg) was placed in a ceramic boat, which was located in the center of a tube furnace. The sample was exposed to a flow of N_2 for 30 min to remove the air from the tube, and then was treated by ammonia at 800°C for 2 h using nitrogen as the carrier gas. After ammonia treatment, the sample was cooled to room temperature and NH_3-treated GA/CMP was obtained.

Material Characterization

The samples were measured by scanning electron microscopy (SEM, Zeiss-Ultra 55), transmission electron microscopy (TEM, Tecnai G2F20S-Twin), X-ray diffraction (XRD, Rigaku D/Max 2400, CuKα radiation, 40 kV, 100 mA, $\lambda = 1.5406$ Å), and X-ray photoelectron spectroscopy (XPS, Axis Ultra Dld, Al Kα radiation, 15 kV, 30 mA). Elemental analyses were carried out using a vario EL cube analyzer. The pore structure was measured by N_2 sorption at 77 K, Brunauer–Emmett–Teller (BET) surface areas were calculated from the isotherm using the BET equation.

Fabrication of Electrodes and Supercapacitor

The active material (80 wt.%), carbon black (10 wt.%), and polytetrafluoroethylene (PTFE, 10 wt.% of a 60 wt.% dispersion in water) were dispersed in ethanol, and then thoroughly mixed in an agate mortar, adding ethanol several times. After that, the mixtures were rolled into a uniform thin film and dried at 80°C for 12 h in a vacuum oven, and then film was cut into 1 cm^2 electrode slice and coated on a slice of nickel foam current collector. Exerted 10 MPa pressure by a table press, the as-prepared electrodes were used as the working electrode. Pt foil and an Hg/HgO electrode were used as the counter electrode and reference electrode, respectively.

Electrochemical Measurement

Electrochemical measurement was performed by using an electrochemical station (CHI660E, CH Instruments, Shanghai) and a three-electrode system in 6 M KOH alkaline electrolyte. The specific capacitances of materials derived from galvanostatic discharge curves were calculated by Equation (1):

$$C_m = \frac{I_d \times \Delta t}{m \times \Delta V} \quad (1)$$

where Δt was the discharge time (s), I_d was the constant discharge current (mA), ΔV was the potential change (excluding ohmic drop IR), m was the mass of active materials in the working electrode when using three-electrode system. In two-electrode system, m was the mass of active material of whole device (mg).

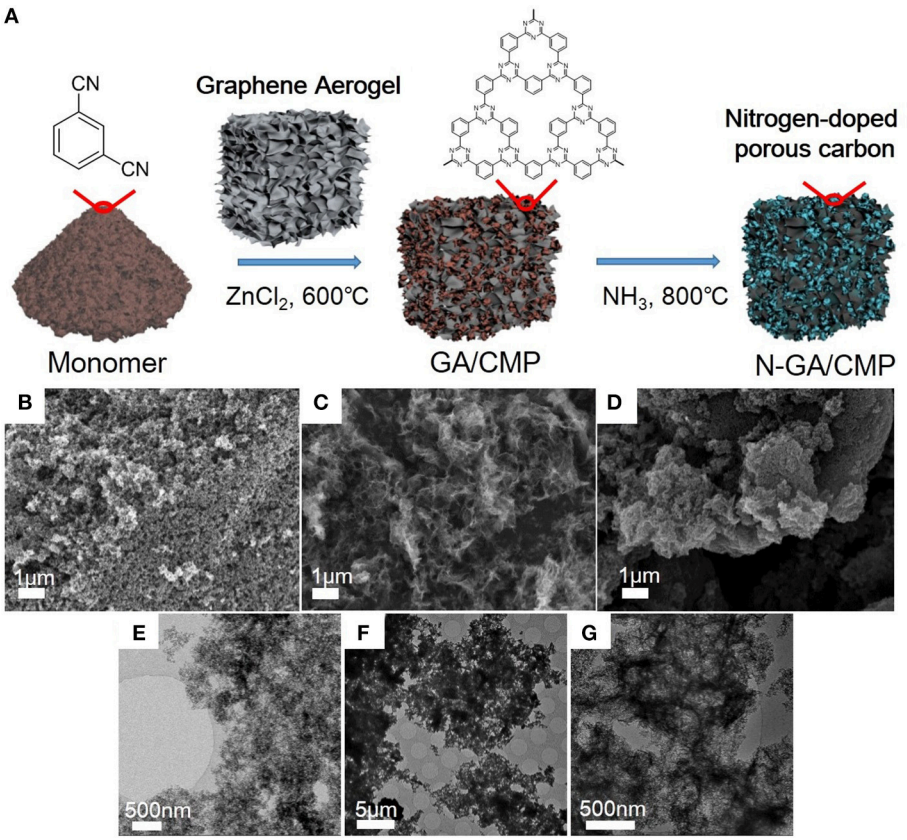

FIGURE 1 | (A) Illustration of synthesis of N-GA/CMPs. **(B–G)** FESEM and TEM images of the CMPs **(B,E)**, GA **(C,F),** and N-GA/CMPs **(D,G)**, respectively.

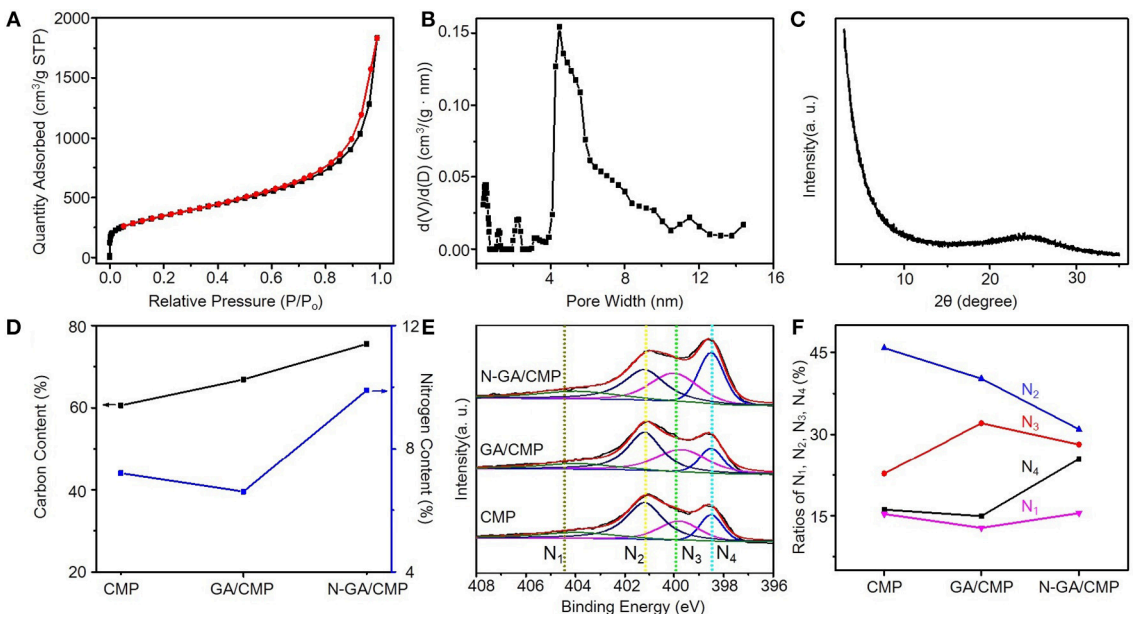

FIGURE 2 | (A) Nitrogen adsorption and desorption isotherms of CMPs (red) and N-GA/CMPs (blue). **(B)** Pore size distribution of CMPs and N-GA/CMPs. **(C)** XRD pattern of N-GA/CMPs. **(D)** EA of N-GA/CMPs for carbon (black) and nitrogen (blue). **(E)** XPS N 1s spectra of CMPs, GA/CMPs and N-GA/CMPs (N_1, oxide nitrogen; N_2, quaternary nitrogen; N_3, pyrrolic nitrogen; N_4, pyridinic nitrogen). **(F)** Ratios of different configurations of nitrogen in the materials.

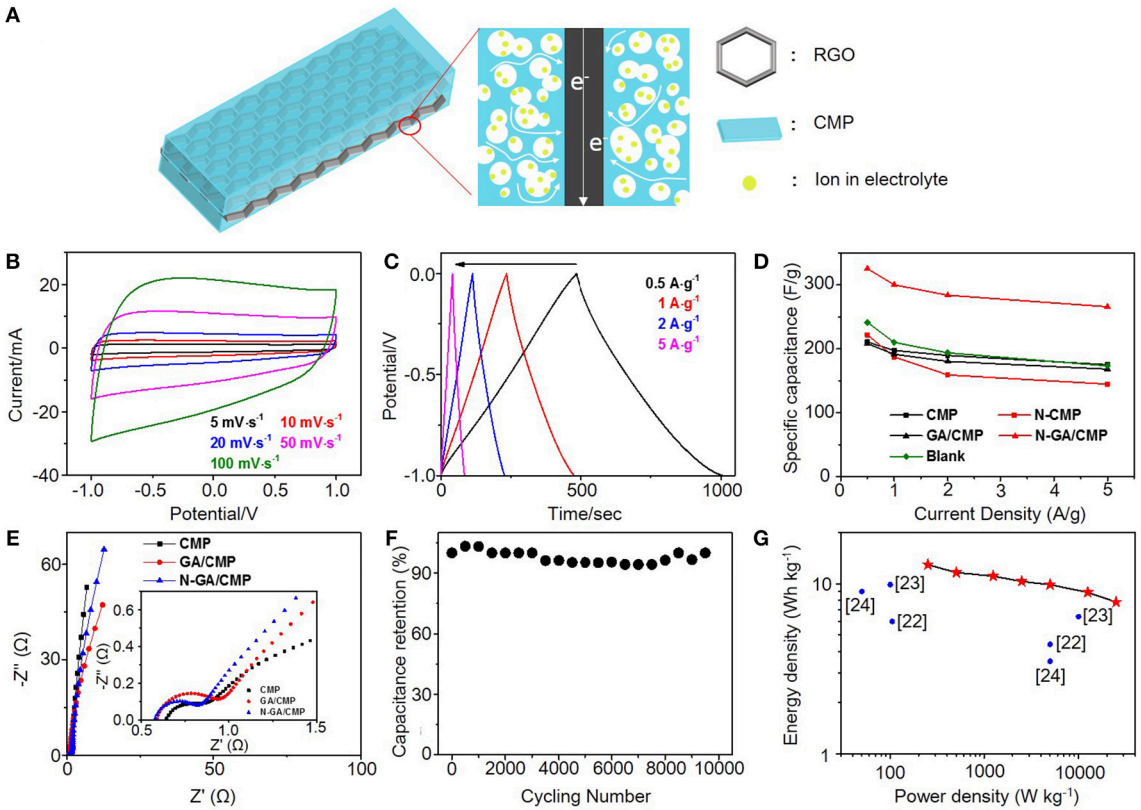

FIGURE 3 | (A) Illustration of the charge transfer in an N-GA/CMPs electrode. **(B)** CV curves and **(C)** GCD curves of the N-GA/CMPs. **(D)** Specific capacitances of CMPs, N-CMPs, GA/CMPs, N-GA/CMPs, GA and physical mixture of 85% CMP and 15% GA as blank. **(E)** Nyquist plots of the CMPs, GA/CMPs and N-GA/CMPs. The insert shows the plots in the high-frequency region. **(F)** Cycling performance of the N-GA/CMPs based supercapacitor. **(G)** Ragone plots of the N-GA/CMPs based two-electrode supercapacitor. The values reported by literatures are shown in the figure.

The energy density (E, W h kg^{-1}) and average power density (P, W kg^{-1}) of the whole two-electrode device were calculated separately by Equations (2, 3):

$$E = \frac{1}{2} \times \frac{C_m \times \Delta V^2}{m \times 3.6} \quad (2)$$

$$P = 3600 \times \frac{E}{\Delta t} \quad (3)$$

RESULTS AND DISCUSSION

After growth (**Figure 1A**), the morphologies of CMPs, GA, and N-GA/CMPs were studied by field emission SEM (FESEM, **Figures 1B–D**) and TEM (**Figures 1E–G**). The FESEM image shows that the CMPs have similar porous structures with the triazine-based CMPs reported in literature (Kuhn et al., 2008b). The TEM image of the N-GA/CMPs shows that the GA skeleton with layered structure is cross-linked and uniformly covered by porous CMPs. Nitrogen adsorption-desorption measurement (**Figures 2A,B**) has been performed to analyze the porous structure of the N-GA/CMPs. The isotherm of the N-GA/CMPs reveals a typical II type, which indicates the combination of micro-pores and meso-pores in the material. The surface area of N-GA/CMPs measured by BET is 1268.5 m^2 g^{-1}, and the powder XRD pattern shows that the N-GA/CMPs don't have any crystallization peaks, proving the amorphous nature (**Figure 2C**).

To further study the chemical structure and elemental composition, N-GA/CMPs were characterized by elemental analysis and XPS. The elemental analysis shows that the pristine GA/CMPs have a 6.3% nitrogen content (**Figure 2D**) (Hao et al., 2014). After carbonization at 800°C in ammonia, the nitrogen content of N-GA/CMPs increases to 9.8%. In order to analyze the nitrogen species in the material, we measured XPS spectra of CMPs, GA/CMPs and N-GA/CMP (**Figure 2E**). The XPS N 1s has four sub-peaks at 398.5, 399.8, 400.9, and 403.1 eV, which represent pyridinic nitrogen, pyrrolic nitrogen, quaternary nitrogen and oxidized nitrogen, respectively. Except quaternary nitrogen, other three types of nitrogen are located at the edges or defects of the CMPs or GA layers. All examples have low percentage of oxidized nitrogen, since the reactions were token place under an inert atmosphere. Notably, after treating at high temperature in ammonia atmosphere, no obvious changes happen on pyrrolic and oxidized nitrogen, while the ratio of quaternary nitrogen decreases and the ratio of pyridinic

nitrogen remarkably increases up to 25.5% (**Figure 2F**), which is of importance for achieving high supercapacitive performance.

To evaluate the supercapacitive performance, cyclic voltammetry (CV), galvanostatic charge–discharge (GCD) tests and electrochemical impedance spectroscopy (EIS) were carried out in a 6M KOH aqueous electrolyte in a conventional three-electrode system (**Figure 3A**). The CV curves for N-GA/CMPs at different scanning rates are shown in **Figure 3B**. All CV curves have quasi-rectangular shape without obvious reduction and oxidation peaks, indicating the N-GA/CMPs have good electroconductivity and stores energy mainly by double-layer energy storage mechanism despise higher content of pyridinic nitrogen. The GCD tests are performed at different current densities from 0.5 to 5 A g^{-1}. The GCD curves (**Figure 3C**) have a triangular shape, consistent with theoretical electrochemical double layer capacitors, and don't have obvious voltage drop, showing the good conductivity of materials. The N-GA/CMPs exhibit the highest specific capacitance of 325 F g^{-1} at the current density of 0.5 A g^{-1}. The calculated specific capacitance values of CMP, GA/CMP and N-GA/CMP (**Figure 3D**) show that the GA cannot greatly increase the specific capacitance, while the high-temperature annealing in ammonia atmosphere leads to a great enhancement. To understand the synergy effect of the GA and the CMPs in the hybrids, we physically mixed same content GA with CMPs and annealed at the same temperature in ammonia atmosphere (named as blank group). The specific capacitance of the physical mixture is nearly same with the CMPs (**Figure 3D**), implying that the increase of specific capacitance mainly results from the chemical combination of porous structure of CMPs and in-plane conductive structure of GA (**Figure 3A**). The CMPs cover on both sides of GA. The interconnected micro-pores and meso-pores of CMPs shorten the diffusion length between external electrolyte and the surface of electrode materials. At the same time, the GA acts as a conductive framework to increase the conductivity of the electrodes.

The Nuquist plot (**Figure 3E**) measured by EIS reveals the device resistance including the electrolyte resistance, the ionic resistance of ions moving through the separator, the intrinsic resistance of the active electrode, and the contact resistance at the interface between the active materials with the current collector. In the high-frequency region, the equivalent series resistance (ESR) of the N-GA/CMPs (0.58 Ω) is smaller than that of CMPs (0.65 Ω) after N-doping, which indicates lower charge transfer resistance at the electrode/electrolyte interface. The smaller radius of semicircular and the more vertical line in the low-frequency region indicate faster ion diffusion in the electrode of the N-GA/CMPs. This phenomenon is attributed to higher ratio of nitrogen in the N-GA/CMPs (Xiang et al., 2015), in agreement with the EA.

In order to test the stability in the application, the N-GA/CMPs were used in a conventional two-electrode system for cycling experiments. The capacitance (**Figure 3F**) remains above 95% after 10,000 charge-discharge cycles at a current density of 5 A g^{-1}. Therefore, the N-GA/CMPs produced by ionothermal synthesis possess not only high supercapacitive performance but also excellent cycling life. The energy density of the N-GA/CMPs supercapacitors (**Figure 3G**) is up to 12.95 Wh kg^{-1}, which is among the highest reported value of the CMP-based supercapacitors (Xu et al., 2017; Yuan et al., 2017; Zhao et al., 2017).

CONCLUSIONS

In summary, GA templated triazine-based CMPs are synthesized by ionothermal method followed by high temperature treatment in ammonia atmosphere. By using GA as the template, the inherent conductivity of triazine-based CMPs is improved. High temperature process in ammonia atmosphere results in higher pyridinic nitrogen content in the GA/CMPs, which introduces more edge sites and defects in the material. As a result, the specific capacitance of N-GA/CMPs electrode increases by 55% up to 325 F g^{-1}, and the energy density reaches 12.95 Wh kg^{-1}. Moreover, there is no significant degradation after 10,000 cycles at a current density of 5A g^{-1}. Considering the easy preparation and outstanding energy storage performance, the N-GA/CMPs show great potential for practical application in high-performance aqueous supercapacitors.

AUTHOR CONTRIBUTIONS

DW designed research. DW, YZ, and YL supervised the project. LP, QG, and ZA performed the experiments. DW and LP wrote the manuscript. All authors commented on the manuscript.

FUNDING

This work was supported by the National Natural Science Foundation of China (51773041, 21603038, 61890940, 21544001), Strategic Priority Research Program of the Chinese Academy of Sciences (XDB30000000), Shanghai Committee of Science and Technology in China (Grant No. 18ZR1404900) and Fudan University.

REFERENCES

Hao, L., Ning, J., Luo, B., Wang, B., Zhang, Y., Tang, Z., et al. (2014). Structural evolution of 2D microporous covalent triazine-based framework toward the study of high-performance supercapacitors. *J. Am. Chem. Soc.* 137, 219–225. doi: 10.1021/ja508693y

Hummers Jr, W. S., and Offeman, R. E. (1958). Preparation of graphitic oxide. *J. Am. Chem. Soc.* 80, 1339–1339. doi: 10.1021/ja01539a017

Kuhn, P., Antonietti, M., and Thomas, A. (2008a). Porous, covalent triazine-based frameworks prepared by ionothermal synthesis. *Angew. Chem. Int. Edn.* 47, 3450–3453. doi: 10.1002/anie.200705710

Kuhn, P., Thomas, A., and Antonietti, M. (2008b). Toward tailorable porous organic polymer networks: a high-temperature dynamic polymerization scheme based on aromatic nitriles. *Macromolecules* 42, 319–326. doi: 10.1021/ma802322j

Lee, J. S. M., Wu, T. H., Alston, B. M., Briggs, M. E., Hasell, T., Hu, C. C., et al. (2016). Porosity-engineered carbons for supercapacitive energy storage using conjugated microporous polymer precursors. *J. Mater. Chem. A*, 4, 7665–7673. doi: 10.1039/C6TA02319C

Li, X. C., Zhang, Y., Wang, C. Y., Wan, Y., Lai, W. Y., Pang, H., et al. (2017). Redox-active triazatruxene-based conjugated microporous polymers for high-performance supercapacitors. *Chem. Sci.* 8, 2959–2965. doi: 10.1039/C6SC05532J

Li, Y., Zhu, H., Shen, F., Wan, J., Han, X., Dai, J., et al. (2014). Highly conductive microfiber of graphene oxide templated carbonization of nanofibrillated cellulose. *Adv. Funct. Mater.* 24, 7366–7372. doi: 10.1002/adfm.201402129

Pang, H., Zhang, Y. Z., Run, Z., Lai, W. Y., and Huang, W. (2015). Amorphous nickel pyrophosphate microstructures for high-performance flexible solid-state electro-chemical energy storage devices. *Nano Energy* 17, 339–347. doi: 10.1016/j.nanoen.2015.07.030

Peng, Y. J., Wu, T. H., Hsu, C. T., Li, S. M., Chen, M. G., and Hu, C. C. (2014). Electrochemical characteristics of the reduced graphene oxide/carbon nanotube/polypyrrole composites for aqueous asymmetric supercapacitors. *J. Power Sourc.* 272, 970–978. doi: 10.1016/j.jpowsour.2014.09.022

Reich, T. E., Behera, S., Jackson, K. T., Jena, P., and El-Kaderi, H. M. (2012). Highly selective CO_2/CH_4 gas uptake by a halogen-decorated borazine-linked polymer. *J. Mater. Chem.* 22, 13524–13528. doi: 10.1039/C2JM31123B

Salunkhe, R. R., Kamachi, Y., Torad, N. L., Hwang, S. M., Sun, Z., Dou, S. X., et al. (2014). Fabrication of symmetric supercapacitors based on MOF-derived nanoporous carbons. *J. Mater. Chem. A*. 2, 19848–19854. doi: 10.1039/C4TA04277H

Wang, G., Zhang, L., and Zhang, J. (2012). A review of electrode materials for electrochemical supercapacitors. *Chem. Soc. Rev.* 41, 797–828. doi: 10.1039/C1CS15060J

Wang, L., Schütz, C., Salazar-Alvarez, G., and Titirici, M. M. (2014). Carbon aerogels from bacterial nanocellulose as anodes for lithium ion batteries. *Rsc Adv.* 4, 17549–17554. doi: 10.1039/C3RA47853J

Wang, Q., Yan, J., Wang, Y., Wei, T., Zhang, M., Jing, X., et al. (2014). Three-dimensional flower-like and hierarchical porous carbon materials as high-rate performance electrodes for supercapacitors. *Carbon* 67, 119–127. doi: 10.1016/j.carbon.2013.09.070

Xiang, Z., Wang, D., Xue, Y., Dai, L., Chen, J. F., and Cao, D. (2015). PAF-derived nitrogen-doped 3D carbon materials for efficient energy conversion and storage. *Sci. Rep.* 5:8307. doi: 10.1038/srep08307

Xie, J., and Zhang, Q. (2016). Recent progress in rechargeable lithium batteries with organic materials as promising electrodes. *J. Mater. Chem. A*. 4, 7091–7106. doi: 10.1039/C6TA01069E

Xu, Y., Jin, S., Xu, H., Nagai, A., and Jiang, D. (2013). Conjugated microporous polymers: design, synthesis and application. *Chem. Soc. Rev.* 42, 8012–8031. doi: 10.1039/C3CS60160A

Xu, Y., Sheng, K., Li, C., and Shi, G. (2010). Self-assembled graphene hydrogel via a one-step hydrothermal process. *ACS Nano* 4, 4324–4330. doi: 10.1021/nn101187z

Xu, Y., Wu, S., Ren, S., Ji, J., Yue, Y., and Shen, J. (2017). Nitrogen-doped porous carbon materials generated via conjugated microporous polymer precursors for CO 2 capture and energy storage. *RSC Adv.* 7, 32496–32501. doi: 10.1039/C7RA05551J

Yuan, K., Zhuang, X., Hu, T., Shi, L., Sfaelou, S., Polnick, U., et al. (2017). 2D Heterostructures derived from MoS2-Templated, cobalt-containing conjugated microporous polymer sandwiches for the oxygen reduction reaction and electrochemical energy storage. *Chem. Electro. Chem*. 4, 709–715. doi: 10.1002/celc.201600850

Yuan, S., Dorney, B., White, D., Kirklin, S., Zapol, P., Yu, L., et al. (2010). Microporous polyphenylenes with tunable pore size for hydrogen storage. *Chem. Commun.* 46, 4547–4549. doi: 10.1039/C0CC00235F

Zhang, L. L., and Zhao, X. S. (2009). Carbon-based materials as supercapacitor electrodes. *Chem. Soc. Rev.* 38, 2520–2531. doi: 10.1039/B813846J

Zhang, Y. Z., Cheng, T., Wang, Y., Lai, W. Y., Pang, H., and Huang, W. (2016). A simple approach to boost capacitance: flexible supercapacitors based on manganese oxides@MOFs via chemically induced *in situ* self-transformation. *Adv. Mater.* 28, 5242–5248. doi: 10.1002/adma.201600319

Zhang, Y. Z., Wang, Y., Cheng, T., Lai, W. Y., Pang, H., and Huang, W. (2015). Flexible supercapacitors based on paper substrates: a new paradigm for low-cost energy storage. *Chem. Soc. Rev.* 44, 5181–5199. doi: 10.1039/C5CS00174A

Zhao, Y., Xie, F., Zhang, C., Kong, R., Feng, S., and Jiang, J. X. (2017). Porous carbons derived from pyrene-based conjugated microporous polymer for supercapacitors. *Micropor. Mesopor. Mater.* 240, 73–79. doi: 10.1016/j.micromeso.2016.10.048

Conflict of Interest Statement: The authors declare that the research was conducted in the absence of any commercial or financial relationships that could be construed as a potential conflict of interest.

Copyright © 2019 Peng, Guo, Ai, Zhao, Liu and Wei. This is an open-access article distributed under the terms of the Creative Commons Attribution License (CC BY). The use, distribution or reproduction in other forums is permitted, provided the original author(s) and the copyright owner(s) are credited and that the original publication in this journal is cited, in accordance with accepted academic practice. No use, distribution or reproduction is permitted which does not comply with these terms.